Asian Journal of Chemistry; Vol. 34, No. 2 (2022), 305-310

ASIAN JOURNAL OF CHEMISTRY

https://doi.org/10.14233/ajchem.2022.23507

Effect of NaBr on the Structural, Thermal and Mechanical Properties of HPMC:NaBr Composite Films

SUNIL KUMAR[1,2], S. RAGHU[3], T. DEMAPPA[4] and J. SANNAPPA[2,*]

[1]Department of Physics, S.S. Arts College and T.P. Science Institute, Sankeshwar-591313, India
[2]Department of P.G. Studies and Research in Physics, Kuvempu University, Jnanasahyadri, Shankaraghatta-577451, India
[3]Department of Physics, K.L.E. Society's, Basavaprabhu Kore Arts, Science and Commerce College, Chikodi-591201, India
[4]Department of Polymer Science, Sir M. Visvesvaraya P.G. Centre, University of Mysore, Tubinakere, Mandya-570017, India

*Corresponding author: E-mail: sannappaj2012@gmail.com

Received: 31 August 2021; *Accepted*: 10 October 2021; *Published online*: 11 January 2022; AJC-20652

The hydroxypropyl methylcellulose (HPMC):sodium bromide (NaBr) composite films were prepared using different concentrations by solution casting method. The crystalline percentage of the pure HPMC was reduced from 74% to 60% upon the incorporation of 0.7 wt.% of NaBr salt, which suggests that the NaBr salt disrupted the host polymer crystalline phase. The two-phase microstructure in the morphological images reflects the phase separation at different concentrations of dopant. The functional studies revealed the considerable variation of intensity and the shift of peaks due to the action of NaBr in the host polymer matrix. The HPMC showed a large increase in the glass transition temperature (T_g) from 65 ºC to 86 ºC and simultaneously reduction in the weight percent loss was observed. The mechanical analysis revealed that the added dopant has a significant effect on the mechanical properties of HPMC.

Keywords: Hydroxypropyl methylcellulose, Sodium bromide, Solution cast method, Thermal property.

INTRODUCTION

The crystallinity of the polymeric material has a big impact on their structural, mechanical and electrical features [1,2]. Understanding of the crystalline nature of a polymer composite is crucial for predicting its suitability in various applications. In most of the recent studies, cellulosic polymer material has been attracting attention as the most abundant resource in nature. Some of the characteristic features are hydrophilicity, biodegradability, reproducibility, non-toxicity and good barrier properties [3]. Cellulose is a potential replacement for petrochemical polymers [4]. Polymers derived from cellulose materials have recently gained the attention of researchers, primarily due to growing environmental concerns and advantages. The advantages include cost-effectiveness, broad availability and post-use processability.

Hydroxypropyl methylcellulose (HPMC) is a derivative of cellulose, likely to be commonly used as an advanced film-shaping and coating material due to its semi-crystalline nature (crystalline and amorphous). The crystalline structures provide solid mechanical backing, whereas the amorphous phase boosts the electric and optical properties in the host polymer [5]. HPMC is soluble in both water and polar organic solvents. It has low moisture barrier properties, which restricts its use in many applications too. However, Ryusuke *et al.* [6] in their study showed that most of the inorganic salts reduce water solubility and moisture content in the host polymer matrix. It is eco-friendly and frequently soluble with a wide variety of metal salts [5,7-9]. In comparison to other inorganic salts, the benefit of using sodium metal particles is their abundance and accessibility at a low cost. Sodium salts are much more reactive, abundant and inexpensive than lithium salts [5,10,11]. There are few sodium-based polymer composites, PPO and PEO with $NaYF_4$, $NaClO_4$, NaI, NaSCN, $NaPF_4$, $NaClO_3$, $NaCF_3SO_4$ and $NaNO_3$ [12,13]. But there are only a few studies available on sodium salts based HPMC composites. Rani *et al.* [5] studied the effects of NaI on the thermal, electrical conductivity and structural properties of the HPMC polymer electrolyte films. Sadeghi [9] studied the effect of NaCl and NaF on the sol-gel transition temperature of hypromellose. The inorganic

compound sodium bromide is widely used source of bromide ions in pharmaceutical preparations [14]. The effect of NaBr on poly(vinyl alcohol) has been studied by Bhargav *et al.* [15], whereas Kumar *et al.* [10] studied the electrochemical cell applications on PEO/PVP/NaBr polymer complex blend electrolytes. Mohapatra *et al.* [11] studied sodium ion-conducting PEO polymer composite films. But no studies have been reported on NaBr based HPMC polymer.

In view of the above importance of HPMC and NaBr salt, the present investigations were carried out to prepare water-soluble (HPMC:NaBr) composite films by using the solution casting method. The prepared films were characterized by various analytical techniques such as XRD, FT-IR, SEM, TGA, DSC and UTM.

EXPERIMENTAL

Sample preparation: Analytical grade sodium bromide and commercial hydroxypropyl methylcellulose (HPMC-E15LV) polymer powder were used in this work. All chemicals were purchased from Sigma-Aldrich. Distilled water was used in this experiment as a solvent. All chemical constituents used were of analytical grade. Polymer composite films were primed by a solution casting method, treating distilled water as a solvent [7].

In this experimental process initially, 3 g of HPMC were added into 100 mL deionized water (3 wt.%), stirring the solution slowly for 30 min with a magnetic stirrer at room temperature (~30 ºC) for clear dissolution. Likewise, a suitable weight percentage ratio (0.1, 0.3 and 0.7 wt.%) was prepared by adding NaBr salt (dissolved) into each prepared 3 wt.% (100 mL) of HPMC polymeric solution under continual stirring for 10 to 12 h. Finally, viscous solutions were transferred into flattened glass plates/petri dishes (10 cm × 15 cm) and kept in a vacuum chamber for evaporation for 5 days. Finally, water as solvent was evaporated slowly at room temperature conditions to achieve the polymer films at the base of glass plates. The film samples were collected in a high-discharge desiccators to prevent dust and moisture uptake. The pure HPMC film and different weight percent ration of NaBr salt were obtained, (S0) HPMC film, (S1) HPMC: 0.1 wt.% NaBr, (S2) HPMC: 0.3 wt.% NaBr, (S3) HPMC: 0.7 wt.% NaBr. The thickness of these films was measured by a screw gauge by measuring the thickness at five different positions and found to be approximately 300 µm.

Characterization: After preparation of HPMC and HPMC:NaBr polymer composite film, samples were evaluated by different experimental techniques, *i.e.* XRD, FT-IR, SEM, TGA, DSC and UTM. The crystallinity study of prepared polymer blend film was assessed by Rigaku Miniflex-II X-ray diffractometer through Ni filtered, Cu*K*α radiation (λ = 1.540 Å). The diffraction peaks were detected at Bragg's angle (2θ) in the limit of 10º-80º with a scanning speed rate of 5º/min and step size of 0.02º. The chemical composition was explored by employing a Fourier transform infrared (FT-IR) with a model-ALPHA BRUKER spectrometer. Analyses were per-formed in the frequency range between 4000-500 cm^{-1} and all spectrums were measured at 4 cm^{-1} resolutions. The surface morphology of prepared films was examined using Carl Zeiss field emission scanning electron microscopy (FE-SEM) at 5 kV and a working distance of approximately 3.5 mm. Before the scan, all film samples were sputter-coated with gold before microscopic analysis. The TGA spectra of HPMC-NaBr film samples (approximately 5 mg of HPMC/NaBr samples were weighted per TGA test) were determined by a DISCOVERY SDT650 TGA, starting with ambient temperatures to 600 ºC with a heating rate of 10 ºC/min. The thermal properties of biopolymer films were studied using the TA instruments, DSC Q20 V24 tool. The heating temperature s from 30 to 390 ºC at 10 ºC/min at a nitrogen gas flow rate of approximately 100 mL/min. The mechanical performance of polymer composite film samples was measured by the Universal Testing Machine (UTM) (ZWICK ROELL Z020). The films were shaped into a rectangular dimension (80 mm × 20 mm × 0.16 mm). The test was done with a load cell of 100N and the drawing speed was pre-set as 12.5 mm/min.

RESULTS AND DISCUSSION

Structural study: The degree of crystallinity has a substantial effect on properties of materials [1,2]. The structural assessment of the prepared composite film samples was carried out by the XRD measurement techniques. In Fig. 1(S), it was witnessed that the pure NaBr salt peaks appeared at between 2θ = 16.58º and 67.06º (PCPDF Card No.: 01-0901, 74-1182 and 72-1539) and several low-intensity peaks were also observed. Very sharp peaks are exhibited at 25º, 30º and 42º suggested the crystalline properties of the NaBr salt. These peaks disappeared in the composite film samples (S1, S2 and S3), which implies that the salt has completely dissolved in the polymer matrices [15-17]. Subsequently for pure HPMC film relatively broad diffraction peaks appeared at around 22.17º (Fig. 1) S0 specifies the semi-crystalline character of HPMC [5,7]. The percentage strength of pure HPMC peaks declined with the raise in the NaBr salt concentration. This was a clear indication of a decrease of the intermolecular interaction (crystalline phase) in the host polymer chain and became an amorphous type film at room temperature. The crystallinity percentage was determined for these films (S0, S1, S2 and S3) using eqn. 1 [18,19]. It was observed from Table-1 that the crystalline degree declined with the loading of NaBr salt [5].

$$X_c = \frac{B_c}{B_c + B_a} \quad (1)$$

where, B_c and B_a are the crystalline and amorphous (halo) provinces, respectively.

FTIR studies: Fig. 2 depicts the FT-IR spectra of pure HPMC and HPMC blended with various wt.% NaBr films (S0-S3). The observed IR characteristic bands correspond to the permitted modes of vibration of various functional groups of HPMC (Table-2) [5,7]. The broad peaks at 3455 and 2336 cm^{-1} in the FT-IR spectra of HPMC are associated with a hydroxyl group (-OH) and the presence of intermolecular hydrogen bonding. The spectrafor complex films (S1, S2 and S3) showed a broadening and shift of the –OH stretching to a lower wave-

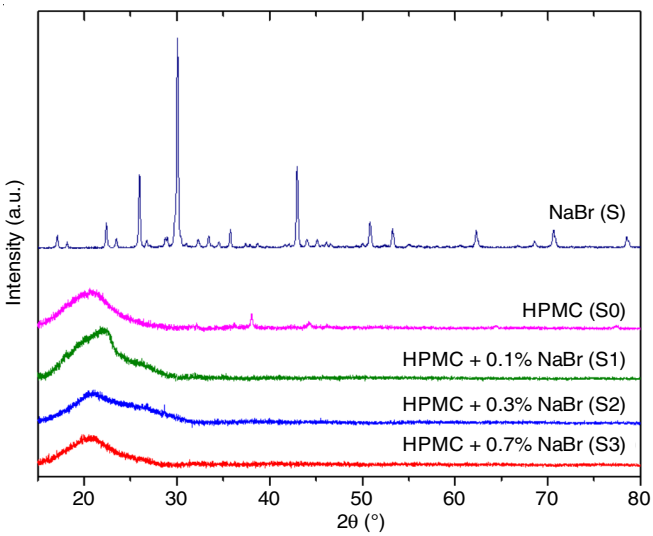

Fig. 1. XRD spectrum of (S) NaBr salt, (S0) HPMC film, (S1) 0.1 wt.% NaBr, (S2) 0.3 wt.% NaBr and (S3) 0.7 wt.% NaBr of samples

TABLE-1
STRUCTURAL PROPERTIES OF HPMC AND HPMC:NaBr

Sample	Sample code	2θ (°)	d-Value (Å)	X_C (%)
Pure HPMC	S0	21.69	4.09	73.83
HPMC:NaBr (0.1 wt.%)	S1	20.58	4.31	73.38
HPMC:NaBr (0.3 wt.%)	S2	21.15	4.19	70.03
HPMC:NaBr (0.7 wt.%)	S3	21.07	4.21	60.27

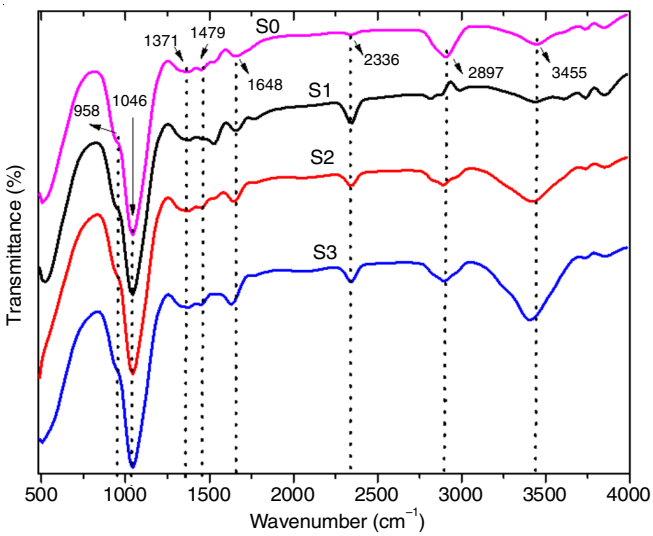

Fig. 2. FT-IR spectrum of pure HPMC and HPMC:NaBr composites

number with the raise of salt concentration in HPMC. Thus, suggesting a greater degree of hydrogen bonding due to the interaction of NaBr salt in the host polymer. An auxiliary large peak for HPMC was observed at 2897 cm^{-1}, which could be due to symmetric stretching of the methyl ($-CH_3$) and hydroxypropyl groups ($-CH_2CH(CH_3)OH$). Simultaneously, a shift in the peak was observed for complex films as a result of band length variation. The peak at 1648, 1479 and 1371 cm^{-1} can be due to the C-O bond stretching within the six-membered cyclic ring asym-metric and symmetric bending vibrations of a methoxy group ($-OCH_3$), respectively. The characteristic peak at 1046 cm^{-1} can be given to C-O-C stretching vibration (S0). The peak at 958 cm^{-1} in the pure HPMC (S0) may be due to the asymmetric pyranose ring and no shift in the peak was observed for the complex films (S1, S2 and S3) (Table-2). In IR spectra, the influence of dopant on vibration modes was noted as a reduc-tion in intensities, broadening of the bands and relocation of the bands to lower wavenumbers. All these differences in the FTIR spectra are strong sign of polymersion complexations in the HPMC:NaBr composites [8,21].

The –OH groups play an important role in directing the crystalline packing [21]. The large shift and variation in the intensity of the –OH group in the complex films cause the crystallization to be interrupted resulting in an increase in the fraction of amorphous content and a decline in the crystallinity percentage. The observed XRD results also show a decline in the crystallinity percentage with increasing salt concentration. Table-2 shows the variations in band location as a function of salt concentration.

Morphology investigation (SEM): SEM is commonly used to investigate the compatibility of the different components of polymer composites by detecting phase separation and interfaces [22]. The mechanical, thermal and ionic conductivity are all affected by the interaction of inorganic dopants with the polymer chain. The surface morphology of the HPMC and HPMC/NaBr films was explored by scanning electron microscopy (SEM). Fig. 3 shows the surface morphology of pure HPMC (S0) and doped HPMC (S1, S2 and S3) films. All NaBr loaded films have the same magnifications. From these SEM micrographs, pure HPMC film shows a plane morphology (S0) [5,7]. The complex polymer composite film samples (S1, S2 and S3) show different degrees of roughness, which confirms that the dopant in the host polymer matrix has segmented. The two-phase microstructure in the SEM reflects the phase separation at different concentrations of NaBr. Thus, morpho-

TABLE-2
KEY FTIR BANDS (cm^{-1}) OF VIRGIN AND LOADED HPMC FILMS

Range (cm^{-1})	Bands	Assignment of bands	Sample code with peaks (cm^{-1})
3,500-3,400	Hydroxyl group	O–H stretching vibration, intermolecular H-bonding	S0-3455, S1-3417, S2-3433, S3-3412
2,900	Methyl and hydroxypropyl group	νCH stretching of methyl and propyl group	S0-2897, S1-2905, S2-2895, S4-2899
2,550-2,500	Hydroxyl group	O–H stretching vibration, intermolecular H-bonding	S0-2336, S1-2335, S2-2339, S3-2340
1,650-1,600	Six membered cyclic	νC–O	S0-1648, S1-1646, S3-1652, S4-1631
1,500-1,450	δCH, δOCH, δCCH	Asymmetric bending vibration of the methyl group in CH_3O	1479 (S0, S1, S2 and S3)
1,400-1,350	Cyclic anhydride	νC–O–C and symmetric bending of a methyl group	1371 (S0, S1, S2 and S3)
1,100-1000	Ethereal C–O–C group	Stretching vibration of C–O–C group	1046 (S0, S1, S2 and S3)
1,000-950	Pyranose ring	ν_{as} of pyranose ring	958 (S0, S1, S2 and S3)

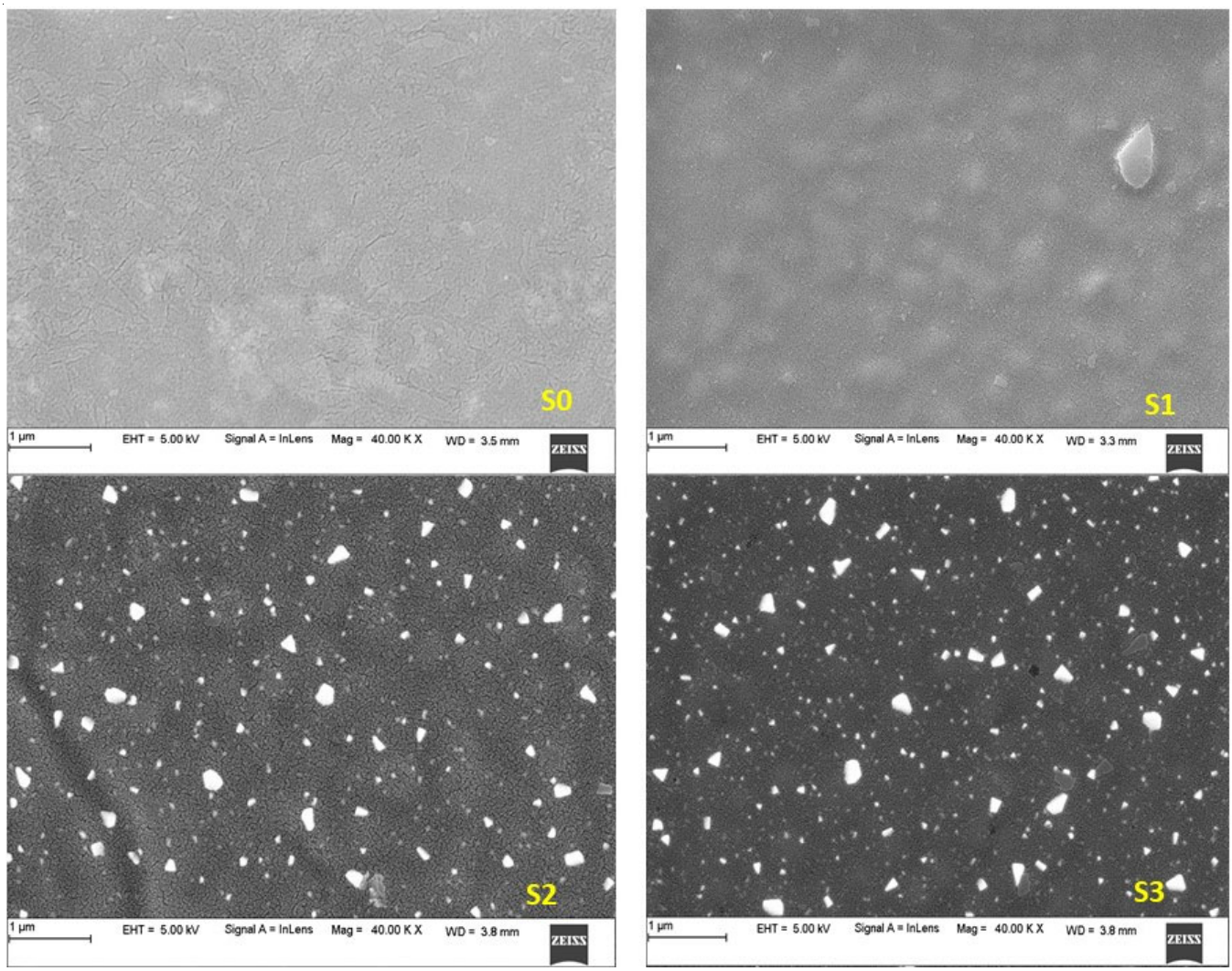

Fig. 3. SEM images of (S0) HPMC, (S1) HPMC: 0.1 wt.% NaBr, (S2) HPMC: 0.3 wt.% NaBr and (S3) HPMC: 0.7 wt.% NaBr

logical reports display that phase segmentation occurs in these complex films [23].

Thermal analysis: Fig. 4 shows the TGA thermograms of the pure HPMC (S0) and NaBr loaded HPMC (S1-S3). The pristine HPMC film showed to be the most thermally stable amongst the cellulose based films such as hydroxy ethyl cellulose (HEC), methylcellulose (MC) and carboxymethyl cellulose (CMC) [24]. The HPMC peak showed two major phases of thermal decomposition, dehydration (I) and decomposition (III) [25,26]. In the first step, pure HPMC TGA curve showed about a 12.55% weight loss in the temperature range of 40-100 ºC. This corresponds to the escape of the physically weak and chemically strong bound H_2O from the polymer matrix. The second step, major weight loss of 78.16% has occurred in the temperature range of 170-370 ºC in pure and complex films. This might be due to the act of NaBr in the host polymer and causes structural decomposition of the polymer systems [24,27].

It should be noted from Table-3 that the peaks of the first decomposition step were insignificant and shifted towards higher temperature with rise in salt concentration. Whereas the second decomposition step peak temperature decreases with

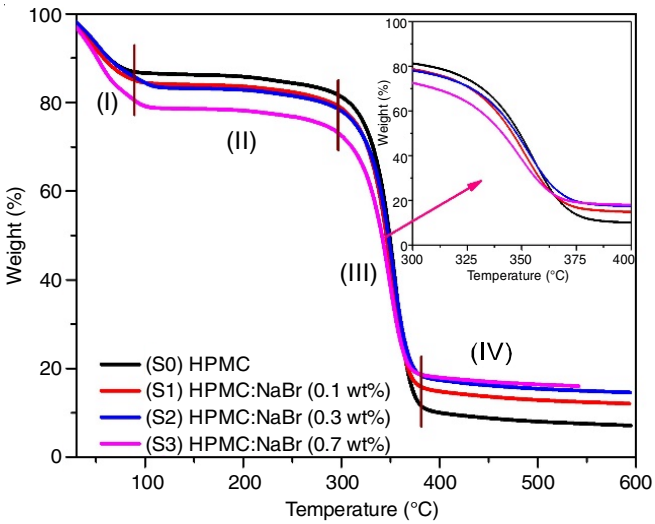

Fig. 4. Thermograms of HPMC (S0), HPMC/NaBr-0.1wt.% (S1), HPMC/NaBr-0.3wt.% (S2) and HPMC/NaBr-0.5 wt.% (S3)

increasing salt concentrations. However, the value of total weight loss decreases with increasing salt concentrations. Conseq-

TABLE-3
THERMAL PROPERTIES OF PURE AND HPMC/NaBr COMPOSITES

Sample code	T_g (°C)	T_d (°C)	Weight loss (%) at different temperature	
			40-100 °C (%)	170-370 °C (%)
S0	65.03	188	12.55	78.16
S1	70.00	181	15.36	71.00
S2	71.28	176	15.45	67.58
S3	88.27	175	19.83	61.88

uently, it can be inferred that the amount of salt increases the amorphous domain in the host polymer, which enhances the thermal stability of the polymer composites.

Differential scanning calorimetry (DSC) analysis: The glass transition temperature of a material helps to fix various flexible and rigid applications [28]. Glass transition temperature (T_g) is a property of amorphous materials or the amorphous component of semi-crystalline materials [29]. At the T_g, the amorphous area undergoes transition from hard to a flexible state resulting in a temperature change from solid to rubbery. The pure HPMC polymer is found in semi-crystalline natures. This type of polymer is thermally depicted by the presence of T_g. It is the transition point between a highly viscous nature and fragile structures known as the glassy state and a viscous, rubbery, silent state and more mobile. The DSC analysis was used to investigate the thermal characteristics of the prepared samples and was carried out between temperature ranges of 30-390 ºC at a rate of 10 ºC/min. The DSC curves of the film samples resulted could be divided into two main regions. The first region between 40 and 100 ºC, corresponds with the volatilization of the water in the film samples and a second one between 180 and 300 ºC corresponds to the depolymerization of the components of the films [24,27]. Fig. 5 shows the pure HPMC film (S0), displaying the glass transition temperature (T_g) at 65.03 ºC. This T_g value is shifted to a higher value with the rise in NaBr salt concentration (S1-S3). The aggregation of inorganic salt in the host polymer reduces the mobility of the polymer chain as a result more energy is required to mobilize the polymer chains, resulting in a larger T_g [30].

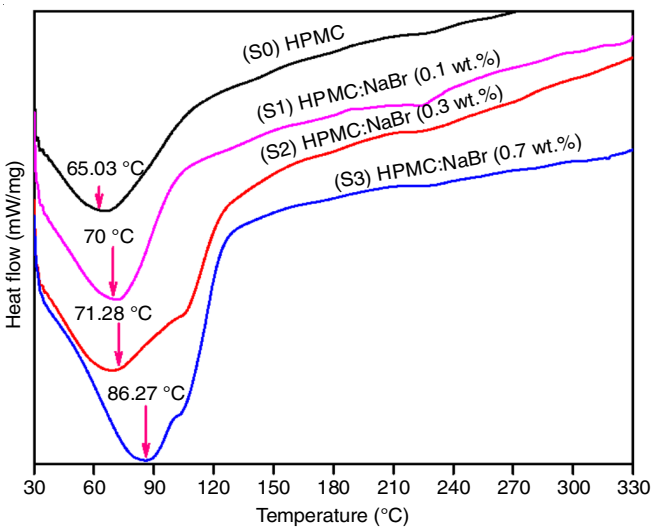

Fig. 5. DSC graph of HPMC and HPMC:NaBr composites

Mechanical properties: Fig. 6 shows the stress-strain curves of HPMC and HPMC with different concentrations of NaBr (S0-S3) composite films. The crystallinity impacts on mechanical properties as its chains linked side-by-side in the crystalline region are tightly bound to each other. As a result, they become more deformable and stiffer as compared to amorphous materials [31,32]. Tensile tests were carried out to define the mechanical behaviour of the polymer matrix, namely the elastic module (Young's module), strength and elongation at break [23,31]. The Young's modulus (YM), tensile strength (TS) and elongation at break (EB) of composite films are calculated (Table-4). The peak value of tensile strength of 37.4 MPa was obtained for the pure HPMC matrix and a decrease in the tensile strength was observed for complex HPMC films. Elastic modulus is a measure of material stiffness. It was clear from Fig. 6 that the modulus value increased with the raise in salt percentage. This can be correlated to the partly exfoliated and partly intercalated morphology of the HPMC composite films observed in SEM. The elongation at break is a measure of the percentage change in the length of the material before fracture. It is a degree of ductility [33]. Elongation at break value of 5.2% was observed for pure HPMC and its value increased to a maximim of 36% for 0.7 wt.% (S3) salt concentration. The observed young's modulus, tensile strength and elongation at break values well correlate with the calculated crystallinity percentage values.

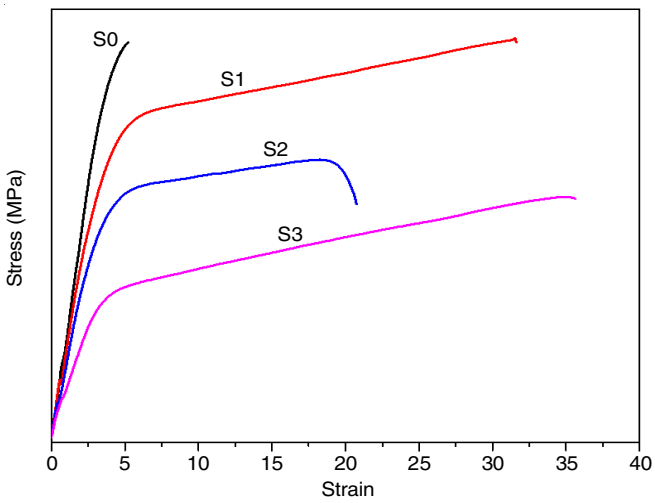

Fig. 6. Stress and strain graph of HPMC and HPMC:NaBr composites

TABLE-4
MECHANICAL PROPERTIES OF HPMC/NaBr COMPOSITES

Sample code	FMAX (N)	Young's modulus (MPa)	Tensile strength (MPa)	Elongation at break (%)	Stress at break
S0	42.42	715	37.4	5.2	37.0
S1	100.34	956	37.0	6.0	32.0
S2	68.91	880	26.1	20.8	21.5
S3	49.21	642	22.7	36.0	21.0

Conclusion

The physical and chemical properties of a HPMC polymer are directly affected by its degree of crystallinity. Salt and host

polymer complexation was confirmed from the XRD and FTIR characterizations. The XRD results showed that by increasing the salt concentration in the host polymer matrix the degree of crystallinity is significantly decreased, because added dopants inhibit the crystallization of polymer chains. SEM images reflects that the degree of roughness increased in composite films compared to the host polymer. The functional studies showed significant variations in the intensity and shift in the peaks, which is the sign of interaction of NaBr with the host polymer matrix. The DSC study showed that in composite films there is rise in glass transition temperature with NaBr concentration, which reveals the interaction of NaBr in the host polymer matrix. Thermogravimetric curve displayed the decrease of weight % loss with an increase in salt concentration, which is attributable to the good thermal stability of complex films as observed from DSC. The tensile test revealed that the degree of crystallinity directly impacts the hardness of a polymeric material. Likewise, the variations in tensile strength, young's modulus and elongation at break were observed. The significant enhancement in amorphocity, high glass transition temperature and large value of elongation at break was observed for the highest doping 0.7 wt.% composite film. The observed mechanical and thermal results are in good agreement with the structural, morphological and functional studies. The hardness and thermal stability of the material suggested that there are scale differences, which may apply to a wide variety of industrial applications.

ACKNOWLEDGEMENTS

One of the authors, Sunil Kumar is thankful to the DST Purse lab, Mangalore University for providing the necessary facilities for the characterization of the samples.

CONFLICT OF INTEREST

The authors declare that there is no conflict of interests regarding the publication of this article.

REFERENCES

1. S.F. Mendes, C.M. Costa, C. Caparros, V. Sencadas and S. Lanceros-Méndez, *J. Mater. Sci*., **47**, 1378 (2012); https://doi.org/10.1007/s10853-011-5916-7
2. Y. Lin, E. Bilotti, C.W.M. Bastiaansen and T. Peijs, *Polym. Eng. Sci*., **60**, 2351 (2020); https://doi.org/10.1002/pen.25489
3. H. Shaghaleh, X. Xu and S. Wang, *RSC Adv.*, **8**, 825 (2018); https://doi.org/10.1039/C7RA11157F
4. R. Weng, L. Chen, S. Lin, H. Zhang, H. Wu, K. Liu, S. Cao and L. Huang, *Polymers*, **9**, 116 (2017); https://doi.org/10.3390/polym9040116
5. N. Sandhya Rani, J. Sannappa, T. Demappa and Mahadevaiah, *Ionics*, **20**, 201 (2014); https://doi.org/10.1007/s11581-013-0952-8
6. T. Ryusuke, M. Reto, L. Jacob, F. Stowasser, C. Stillhart and S. Page, *Mol. Pharm*., **17**, 2768 (2020); https://doi.org/10.1021/acs.molpharmaceut.9b01109
7. S. Sharma, T.N. Ansari and S. Handa, *ACS Sustain. Chem. Eng.*, **9**, 12719 (2021); https://doi.org/10.1021/acssuschemeng.1c04607
8. N. Sandhya Rani, M.S. Manjunatha, J. Sannappa and T. Demappa, *Mater. Today: Proc*., **5**, 22543 (2018); https://doi.org/10.1016/j.matpr.2018.06.626
9. E. Sadeghi, Masters of Science Thesis, Effect of Strong Electrolyte Containing Gelling Aids on the Solgel Transition Temperature of Hypromellose 2910, Department of Biomedical Engineering, The University of New Mexico, Albuquerque, New Mexico, USA (2018).
10. K.K. Kumar, M. Ravi, Y. Pavani, S. Bhavani, A.K Sharma and V.V.R. Narasimha Rao, *J. Memb. Sci*., **454**, 200 (2014); https://doi.org/10.1016/j.memsci.2013.12.022
11. S.R. Mohapatra, A.K. Thakur and R.P. Choudary, *Ionics*, **14**, 255 (2008); https://doi.org/10.1007/s11581-007-0171-2
12. T. Sreekanth, M.J. Reddy, S. Ramalingaiah and U.V. Subba Rao, *J. Power Sources*, **79**, 105 (1999); https://doi.org/10.1016/S0378-7753(99)00051-8
13. S.S. Rao, M.J. Reddy, E.L. Narsaiah and U.V. Subba Rao, *Mater. Sci. Eng. B Solid State Mater. Adv. Technol.*, **33**, 173 (1995); https://doi.org/10.1016/0921-5107(94)01206-7
14. M.J. Dagani, H.J. Barda, T.J. Benya and D.C. Sanders, Bromine Compounds, In: Ullmann's Encyclopedia of Industrial Chemistry, Wiley-VCH: Weinheim (2000).
15. P.B. Bhargav, V.M. Mohan, A.K. Sharma and V.V.R.N. Rao, *J. Appl. Polym. Sci.*, **108**, 510 (2008); https://doi.org/10.1002/app.27566
16. F. Ahmad and E. Sheha, *J. Adv. Res*., **4**, 155 (2013); https://doi.org/10.1016/j.jare.2012.05.001
17. Ismayil, V. Ravindrachary, R.F. Bhajantri, P.S. Dhola and G. Sanjeev, *Nucl. Instrum. Methods Phys. Res. B*, **342**, 29 (2015); https://doi.org/10.1016/j.nimb.2014.09.021
18. P.H. Hermans and A. Weidinger, *Macromol. Chem. Phys.*, **44-46**, 24 (1961); https://doi.org/10.1002/macp.1961.020440103
19. Sangappa, T. Demappa, Mahadevaiah, S. Ganesha, S. Divakara, M. Pattabi and R. Somashekar, *Nucl. Instrum. Methods Phys. Res. B*, **266**, 3975 (2008); https://doi.org/10.1016/j.nimb.2008.06.021
20. Y. Prakash, H. Somashekarappa, A. Manjunath, M. Mahadevaiah and R. Somashekar, *Adv. Mater. Res*., **2**, 37 (2013); https://doi.org/10.12989/amr.2013.2.1.037
21. E. Sjostrom, Wood Chemistry: Fundamentals and Applications, Academic Press: New York, pp. 169-189 (1981).
22. P.P. Chu and M.J. Reddy, *J. Power Sources*, **115**, 288 (2003); https://doi.org/10.1016/S0378-7753(02)00717-6
23. S. Zhang, J.Y. Lee and L. Hong, J. Power Sources, 126, 125 (2004); https://doi.org/10.1016/j.jpowsour.2003.08.011
24. X.-G. Li, M.-R. Huang and H. Bai, *J. Appl. Polym. Sci.*, **73**, 2927 (1999); https://doi.org/10.1002/(SICI)1097-4628(19990929)73:14<2927::AID-APP17>3.0.CO;2-K
25. C. Cozic, L. Picton, M.R. Garda, F. Marlhoux and D. Le Cerf, *Food Hydrocolloids*, **23**, 1930 (2009); https://doi.org/10.1016/j.foodhyd.2009.02.009
26. M.J. Zohuriaan and F. Shokrolahi, *Polym. Testing*, **23**, 575 (2004); https://doi.org/10.1016/j.polymertesting.2003.11.001
27. E.M. Abdelrazek, I.S. Elashmawi, A. El-khodary and A. Yassin, *Curr. Appl. Phys.*, **10**, 607 (2010); https://doi.org/10.1016/j.cap.2009.08.005
28. J.W. Nicholson, The Chemistry of Polymers, RSC Publishing: Cambridge, UK, Ed.: 3. pp. 46-53 (2006).
29. A. Shrivastava. Introduction to Plastics Engineering (A volume in Plastics Design Library), Elsevier, pp. 1-16 (2018).
30. M. Persson, G.S. Lorite, S.-W. Cho, J. Tuukkanen and M. Skrifvars, *ACS Appl. Mater. Interfaces*, **5**, 6864 (2013); https://doi.org/10.1021/am401895f
31. N. Reddy and Y. Yang, *Trends Biotechnol.*, **23**, 22 (2005); https://doi.org/10.1016/j.tibtech.2004.11.002
32. K. Balani, V. Verma, A. Agarwal and R. Narayan, Biosurfaces: A Materials Science and Engineering Perspective, John Wiley & Sons Inc. (2015).
33. S.R. Djafari Petroudy, Physical and Mechanical Properties of Natural Fibers, In: Advanced High Strength Natural Fibre Composites in Construction, Woodhead Publishing, pp. 59-83 (2017).